



## An innovative concrete-steel structural system for long-span structure allowing a fast and simple erection

Clemence Lepourry, Piseth Heng, Hugues Somja, Nicolas Boissonnade, Franck Palas

### ► To cite this version:

Clemence Lepourry, Piseth Heng, Hugues Somja, Nicolas Boissonnade, Franck Palas. An innovative concrete-steel structural system for long-span structure allowing a fast and simple erection. Structures, 2019, 21, pp.55-74. 10.1016/j.istruc.2019.04.016 . hal-02372370

**HAL Id: hal-02372370**

**<https://hal.science/hal-02372370>**

Submitted on 20 Jul 2022

**HAL** is a multi-disciplinary open access archive for the deposit and dissemination of scientific research documents, whether they are published or not. The documents may come from teaching and research institutions in France or abroad, or from public or private research centers.

L'archive ouverte pluridisciplinaire **HAL**, est destinée au dépôt et à la diffusion de documents scientifiques de niveau recherche, publiés ou non, émanant des établissements d'enseignement et de recherche français ou étrangers, des laboratoires publics ou privés.



Distributed under a Creative Commons Attribution - NonCommercial 4.0 International License

# An innovative concrete-steel structural system for long-span structure allowing a fast and simple erection

C. Lepourry<sup>a,b\*</sup>, P. Heng<sup>a,b</sup>, H. Somja<sup>a</sup>, N. Boissonade<sup>c</sup> and F. Palas<sup>b</sup>

<sup>a</sup> National institute of applied sciences, Department of Civil Engineering, Rennes, France

<sup>b</sup> INGENOVA, Civil Engineering Office, Rennes, France

<sup>c</sup> Laval University, Civil and Water Engineering Department

\* Corresponding author: [clemence.lepourry@insa-rennes.fr](mailto:clemence.lepourry@insa-rennes.fr)

## Abstract

In achieving medium-to-long span slab, steel-concrete composite beams may offer an alternative over pre-stressed beams for the so-called disadvantages of the latter; for example the heavy weight of pre-stressed beams makes their handling expensive. However, the use of composite beams by concrete builders is still limited due to the lack of specific tools and skills for on-site erections and the need for a supplementary fire protection. This article presents an innovative steel-concrete moment resisting portal frame that overcomes these difficulties. It is composed of composite tubular columns, and a composite beam made of a U-shape steel profile used as permanent formwork to encase a concrete beam. The steel-concrete duality of the proposed beam allows an erection on site without any weld or bolt by a wise positioning of the construction joints. As only steel elements have to be handled on site, there is no need of heavy cranes. This system has been used to build a research center near Rennes, in France. As it is not covered in present norms, an experimental validation was required. In this paper, a series of full-scale experimental tests that have been performed in order to assess the global and the local behaviour of the frame and its connections are presented. A series of asymmetrical push-out tests were carried out in order to determine the ductility and resistance of shear connectors; one 4-point bending test was made to investigate the resistance under sagging bending moment; and, two tests of the beam-to-column joint were performed in order to validate a strut and tie design model of the joint. Finite element simulations have also been made in order to acquire more information for the development of the analytical models.

**Keywords:** Hybrid concrete-steel beam, Innovative construction, U-shape steel profile, L-shape shear connector, beam-to-column joint, full-scale experimental test.

## 1. Introduction

In usual concrete buildings, medium-to-long span slabs can only be achieved by using prestressed beams. However, these elements are heavy, making their handling expensive; the cladding of these beams to vertical elements creates several difficulties, particularly in case of moment resisting frames; at last, their precamber implies a cautious management of the concreting and is a source of defects. Steel-concrete composite beams may offer an alternative, with similar performances [1]. However, they are not considered by concrete builders, because specific tools and skills are needed to erect them on site and to make connections between members. Moreover, usual composite members require a supplementary fire protection, which is costly and unsightly.

This article presents an innovative steel-concrete moment resisting portal frame that overcomes these difficulties. It is based on composite tubular columns, and composite beams composed of a U-shape steel profile used as permanent formwork to encase a concrete beam as seen in Fig. 1. It is named U-shape concrete-steel hybrid beam (UCSB).



Fig. 1. U Shape Concrete-Steel Hybrid Beam

Similar systems have been developed in the past. Uy et al.[2,3] studied the behaviour of a U-profile composite beam with concrete infill made of concrete, profiled sheeting and additional positive reinforcement. In this beam, the shear resistance is achieved exclusively by the friction between the profile and the inside concrete. The objective was to compare the flexural resistance of that new type of beams compared to the same concrete-section. Nakamura in [4] and Park et al in [5] proposed U-shape steel girders with concrete infill in order to increase flexural resistance and stiffness of the traditional composite beams. These two composite beams are composed of a U-shape steel girder connected to the reinforced concrete slab at its inward upper flanges by shear headed studs. More recently, Chen et al in [6] developed a checkered U-shape steel plate girder in order to increase the longitudinal shear resistance between steel and concrete so that the number of shear studs could be reduced. In all these solutions, an additional bracing of the U-shape steel profile is necessary in order to obtain sufficient resistance for the lateral torsional buckling. In the solution proposed by Liu et al [7], the longitudinal shear

resistance is obtained by the use of L-angle shear connectors (transversal steel elements) that are welded to the two upper flanges. These connectors also have a role to maintain the shape of the U profile and avoid its lateral buckling. However, no reinforcement rebars have been included in the concrete beam drop. This leads to its inefficiency in resisting flexural and fire loading.

55 In the proposed UCSB, the concrete beam drop is reinforced. In this regard, the UCSB can be considered as a dual member: it is the addition of a composite beam (steel plus concrete) and of a reinforced concrete beam. Adding rebars in the concrete section contributes to the increase of both the flexural and shear resistance of the UCSB. Furthermore, the resistance of the UCSB to fire can be ensured by the inside reinforced concrete beam, making it unnecessary for any additional fire protection. The association of the two beams also gives a convenient  
60 solution adapted to concrete builders. Indeed, on-site joints of the UCSB can be designed to be made exclusively by the inside concrete element.

Since handling steel parts of the UCSB on-site is light, there is no need for heavy cranes on site. This practicality of the UCSB has been decisive in the choice of the hybrid portal frame for its first application, i.e. the construction of the AVRIL headquarters in Rennes, France (Fig. 2). This building is a circular ring with an external  
65 circumference of 80 m. It is three-storey high, and the structural skeleton is composed of ninety moment resisting hybrid portal frames. The length of the frame is 13.5m and its height is 2.35m as seen in Fig. 3.



Fig. 2. Picture of the AVRIL construction site

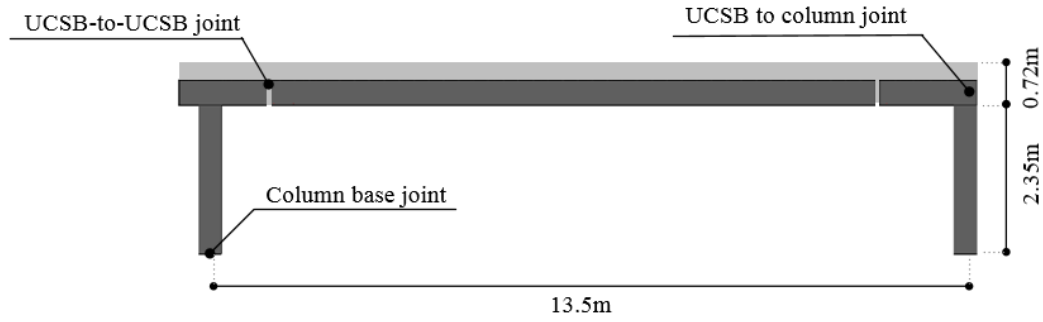


Fig. 3. The hybrid portal frame and its typical joints

Columns are concrete filled steel tubular columns. The beam-column joint is welded and has been made in the workshop. On-site joints are made at the inflection point of the bending moment diagram in the beam. As moments in these joints are low, the assembly is made by the concrete and the steel sections do not have to be connected. In the same way, the column base joint is hinged and is designed to transfer loads exclusively by the inside concrete column. As a consequence, the steel portal frame is divided in three elements prefabricated in the workshop: the central part of the beam, and the two outer parts made of the columns welded to the hogging zone of the beam as seen in Fig. 4. These parts have not to be connected by bolts on site, and the concrete workers can then set up these elements without any difficulty, as a usual formwork.

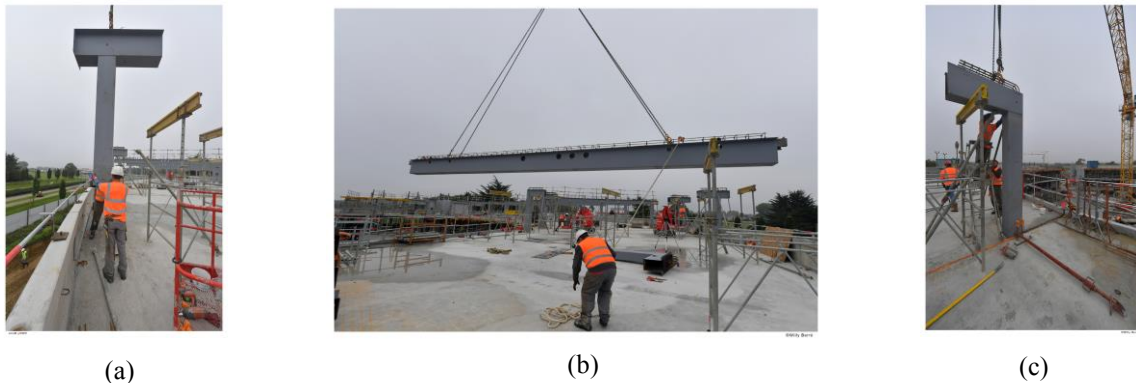


Fig. 4. Components of the hybrid frame (a) outer part 1. (b) Central part. (c) Outer part 2.

This paper presents the investigations made on the behaviour of the portal frame. In a first part, the global analysis of the hybrid frame that was performed with a specific software called HBCOL [8] in order to obtain the distribution of the forces in the frame is presented. Then, the article focuses on the investigations over the behaviour of the different components of the hybrid frame. Firstly, the behavior of L-angle connectors in the UCSB has been studied by performing 4 asymmetric push-out tests. These tests were used to validate a FE model. An analytical expression of the shear resistance was then proposed based on the results obtained from a numerical parametric study. Furthermore, the global behaviour of the UCSB was studied by a six-point flexural test. The

results of these tests were also used to validate the application of the software HBCOL for UCSB elements in sagging. Then, the different joints of the frame have been designed. Two experimental tests have been carried out on the UCSB-to-UCSB joint in order to validate the design. The behavior of the UCSB-to-column joint was verified by four full-scale experimental tests. A detailed finite element model has been validated and has been used to calibrate the analytical model of the joint. Details of the columns base joint are also presented. Finally, a feedback of the first application of the hybrid frame is provided at the end of the paper.

## 2. Structural analysis and design of the portal frame

### 2.1 Description of the members

The configuration of the portal frame has been described in the previous paragraph. The beam consists in a U-shape steel profile filled with reinforced concrete, a reinforced concrete slab and shears connectors, which are detailed in Fig. 5. The U-shape steel profile is made of cold-formed steel with a thickness of 6 mm. The lower flange is 300 mm wide, the two webs are 500 mm high, and the two upper flanges are 100 mm wide. The height of the slab deck is 220mm and its effective flange width is 3300mm. This effective width depends on the beam span and bending moment diagram, and is computed based on the method in Eurocode 4, part 1-1 [11]. The composite mechanism of the UCSB is ensured by L-angles welded to the upper flanges of the steel profile. The dimensions of the L-angle connectors are 40x40x4mm and their spacing is 300mm. Steel rebars inside the UCSB are detailed in Fig. 5 (b) and (c). The spacing of the stirrups is given in the detailed description of the reinforcement schemas in Appendix A.

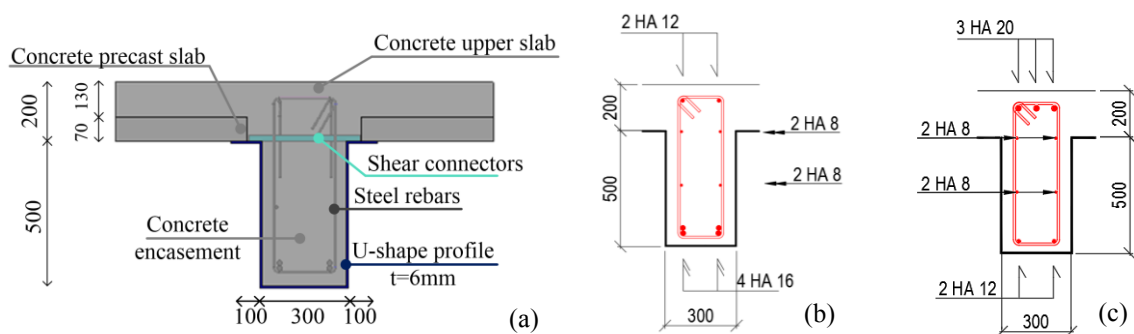


Fig. 5. UCSB - (a) Cross section. (b) Reinforcement bars of central part. (c) Reinforcement bars of outer parts.

On the other hand, the composite column is made of a rectangular hollow steel column with a thickness of 10mm filled with reinforced concrete and four HA12 steel rebars, as seen in Fig. 6. The width and the height of the cross-section are 300 and 400mm.

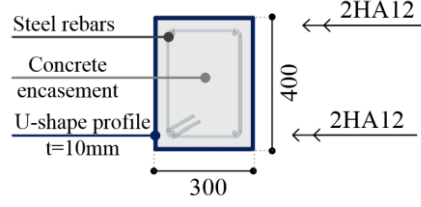


Fig. 6. Composite columns: Cross section and reinforcement bars.

The nominal values of yield strength ( $f_y$ ) for L-angle, U-shape profile and rectangular hollow steel columns are 235 MPa, 355 MPa and 355 MPa, respectively. In addition, the steel grade of the steel reinforcement bars is B500B with a partial factor being 1.15. The concrete has a strength class of C25/30 with a partial factor being equal to 1.5.

## 2.2 Structural analysis of the portal frame

The structural analysis of the portal frame was performed using an FE-based software called HBCOL, in order to determine the distribution of the internal forces in the members, and the forces applied on the joints. This software, developed by Keo et al. [7] is able to take into account the material and geometrical non-linearity as well as the effect of partial shear connection. It is based on a plane beam finite element formulation written in a corotational framework.

The concrete is modelled using the expression provided by EN1992-1.1 [9] (Fig. 7 (a)). The behaviour in tension is however neglected. Furthermore, elastic-perfectly-plastic stress-strain relationships based on EN1992-1.1 and EN1993-1.1 [9,10] were used for steel rebars and steel U-shape profile (Fig. 7 (b) and (c)). For shear connectors, the stress-strain relationship adapted with force-slip experimental curves (Fig. 7 (d)) is used. It will be described in a following paragraph.

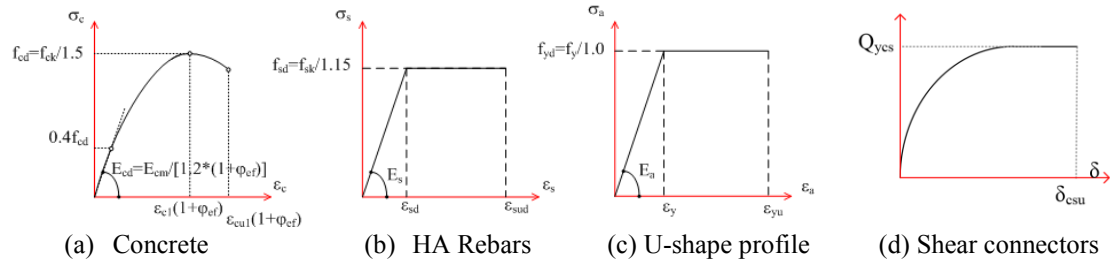


Fig. 7. : Strain stress relationship for UCSB components

## 2.3 Design of the portal frame

120 The bending moments and shear forces obtained at ULS are presented in Fig. 8 (a) and (b).

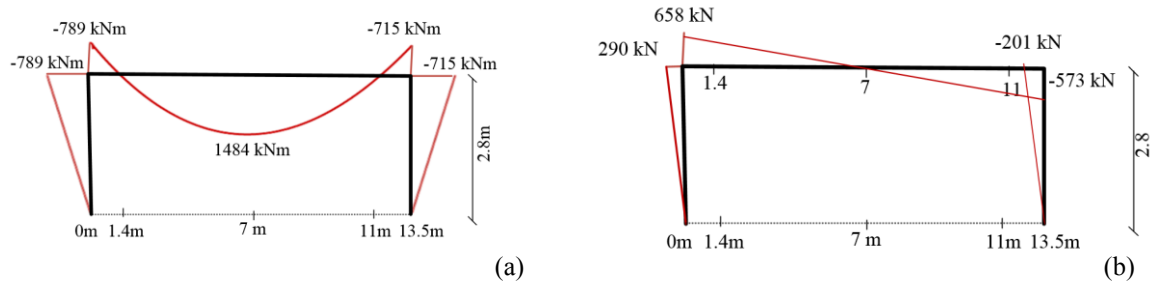


Fig. 8: (a). Applied bending moments at ULS. (b). Applied shear forces at ULS.

From these diagrams, the columns were designed following EN1994-1.1 [11], whereas the hypothesis of Bernoulli was adopted for the design of the beam. The distribution of the shear forces between the web of the U-shape profile and the stirrups in the concrete had also to be determined. This was made by computing the bending moments in the concrete and in the steel from stresses resulting of finite element analysis and by deriving them in order to obtain the distribution of the shear forces between materials. The cross-section of the beam and of the columns as well as the reinforcements bars, detailed in Section 2.1, were obtained from this design.

125 The displacements and the slips along the beam are given in Fig. 9 (a) and (b), respectively. The maximal deflection at mid-span is 31.2mm. It does not exceed the limit  $L/250$  given by EN1992-1.1 [9]. The slip at the concrete-steel interface is moderate. It is less than 1.5mm. It can be observed that the slips of the outer parts of the beam are almost equal to zero because the longitudinal shear resistance in these parts is much larger, due to the specific detailing of the on-site joints.

130 beam are almost equal to zero because the longitudinal shear resistance in these parts is much larger, due to the specific detailing of the on-site joints.

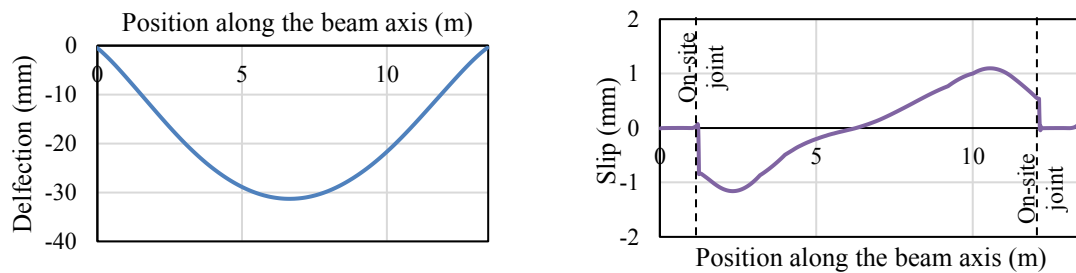


Fig. 9. SLS solicitations along the beam. (a) displacement (b) slips



### 3. Behaviour of L angle shear connectors of UCSB

Headed shear stud connectors are usually chosen in many composite beams [12-15], however, they are not suitable in the case of UCSB due to the thickness of the U-shape steel profile. With such a regard, L-angle steel elements are chosen as an alternative. Welded to the two upper edges of the U-shape steel profile (Fig. 5), these shear connectors not only have the role to transfer the force between the two materials, but also serve to maintain the shape of the steel cross-section during concrete casting. Due to the fact that this new type of shear connectors are not covered by the present norms, an experimental program and numerical simulations have been performed in order to determine their behavior. These are presented in this section.

#### 3.1 Experimental program

Four asymmetrical push-out tests have been performed in order to determine the behaviour of the L-angle shear connectors. They have been described in detail by Keo et al [16]. These tests were inspired from the works presented in [17,18].

The test setup consists of a jack machine with a capacity of 1500kN, a UCSB specimen, vertical supports and a bracing system as seen in Fig. 10. A horizontal load was applied by the jack machine to the specimen through a steel element that is connected to the U-shape steel profile. At the other end of the specimen, the back side surface of the concrete floor was put in contact with a rigid steel beam that gives reaction against the loading.

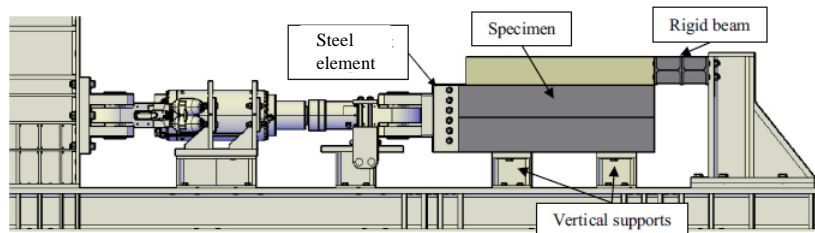


Fig. 10. Push-out test setup

The cross-section of the UCSB is the same as the one of the AVRIL project (see Fig. 5) except that the width and the height of the slab are 1300mm and 200mm, respectively. The length of the specimen is 1200 mm.

In the first specimen, denoted by "L<sub>40</sub>", the steel-concrete shear connection is made by three L-angles with a dimension of 40x40x4 mm. In the other three specimens, denoted by "L<sub>50-I</sub>", "L<sub>50-II</sub>" and "L<sub>50-III</sub>", the connection is ensured by three L-angles with a dimension of 50x50x5 mm. The L-angle connectors are fixed to the upper flanges of the U-shape profile over a length of 40mm by a peripheral fillet weld with an effective thickness of 4mm. The

contact surfaces between the U-shape steel profile and the concrete block are greased in order to distribute shear forces exclusively to the shear connectors.

The cast-in-place concrete block and the precast concrete slab are made of a concrete type of C25/30 and C40/45, respectively. The concrete characteristics at the day of the test were determined on cylinder samples with a dimension of 11×22 cm. The steel grade of the U-shape steel profile and L-shape shear connectors are S355 and S235. Coupon samples were taken from the steel sheet and from the shear connector used in the push-out specimens. The results of the material characteristic tests are summarized in Table 1. The test was made at an early age of the concrete in order to get a concrete resistance between 60 and 80 % of the characteristic value.

Table 1 : Mean materials properties

	Concrete		U-shape		Connectors	
	Beam and slab	Precast slab				
	$f_{cm}$ (MPa)	$f_{cm}$ (MPa)	$f_y$ (MPa)	$f_u$ (MPa)	$f_y$ (MPa)	$f_u$ (MPa)
L <sub>40</sub>	27	43	450	510	430	550
L <sub>50-I</sub>	20	33.5			320	449
L <sub>50-II</sub>	21.5	34.9				
L <sub>50-III</sub>	22.7	42.5				

The loading procedure was divided into two steps based on the recommendations given in EN1994-1.1 [11]. In the first step, 25 loading/unloading cycles between 5 and 40 % of the ultimate load were applied. The load was then applied up to the failure.

### 3.2 Test results

The force-slip and the force-uplift curves for each test are illustrated in Fig. 11. The maximum load ( $P_{max}$ ), the ultimate slip ( $s_u$ ) and the ultimate uplift ( $\delta_u$ ) have been computed as indicated in EN1994-1.1[11], and are reported in Table 2.  $S_u$  and  $\delta_u$  are the values of the slip and the uplift corresponding to a load equal to 80% of  $P_{max}$  after the peak.

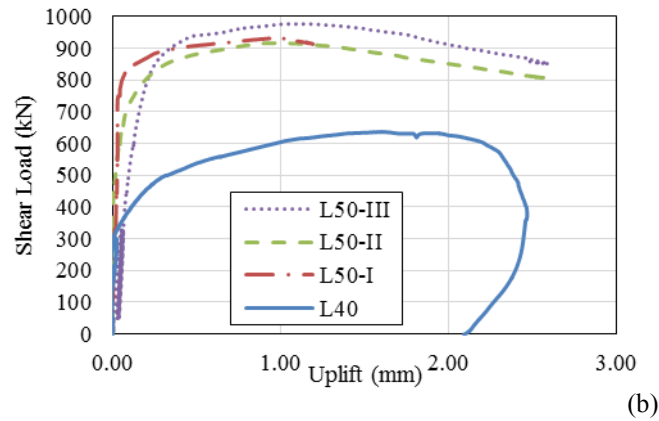
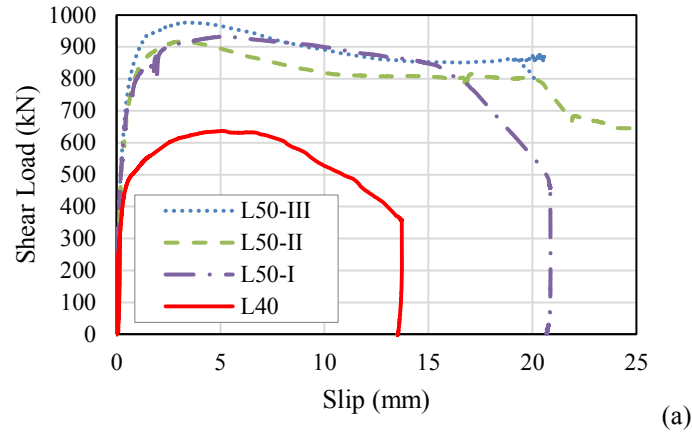


Fig. 11. Experimental curves load-mean slip (a)/uplift (b)

Table 2 : Results of push-out tests

	L <sub>40</sub>	L <sub>50-I</sub>	L <sub>50-II</sub>	L <sub>50-III</sub>
$P_{\max}$ (kN)	212	310	305	325
$s_u$ (mm)	8.22	14.22	8.63	17.44
$\delta_u$ (mm)	1.44	1.5	2.5	2

As the ultimate slips are larger than 6 mm, L-angle shear connectors can be considered as ductile, following EN1994-1.1 [11]. Besides, the ultimate uplift between concrete and steel is smaller than half of the longitudinal slip. Consequently, the shear connectors have a sufficient capacity in resisting the vertical separation between the concrete component and the steel beam.

During experimental tests, cracks were not observed on the concrete slabs. After the tests, the concrete was removed in order to examine the condition of the connectors as seen in Fig. 12. The failure of shear connectors occurred near the zones welded to the upper flanges.



Fig. 12. Angle deformations after testing

### 3.3 Design equation for L angle shear connectors

In order to develop a design equation for L-angle shear connectors, a numerical simulation is performed in ABAQUS. The detailed description of this model was presented by Keo et al [16]. The FE model was first validated with the experimental results. The comparisons of the load-slip and load-uplift curves between results obtained from the experiments and the FE model are illustrated in Fig. 13 for specimens L50s and in Fig. 14 for specimen L40. It is shown that the FEA model successfully predicted the shear capacity and the initial stiffness of the L-shaped shear connectors. However, the prediction of the post yield behavior is poor. It should be also noted that this validation is made only on test specimens with similar properties. More experimental tests on specimens with different properties should be done in order to enrich this validation.

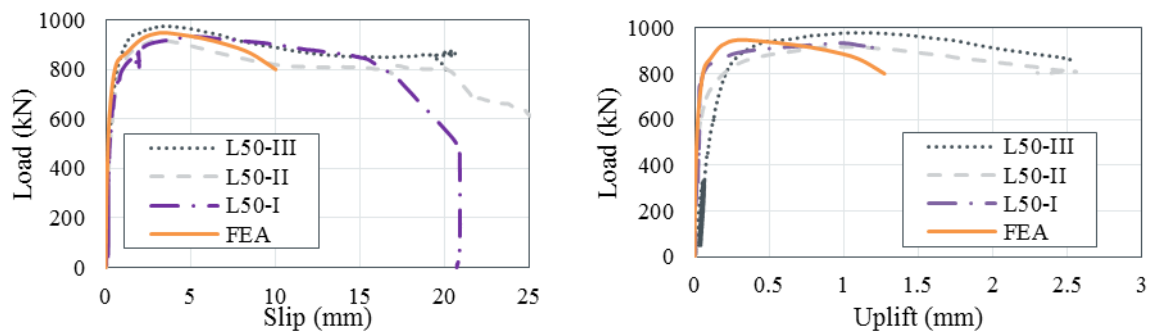


Fig. 13. Comparison of FEA against experimental results of L<sub>50</sub>-I, L<sub>50</sub>-II, L<sub>50</sub>-III specimen

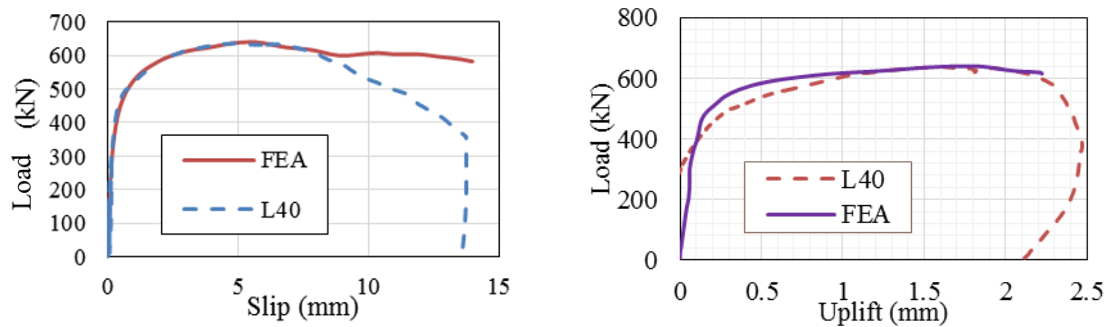


Fig. 14. Comparison of FEA against experimental results of L<sub>40</sub> specimen

Fig. 15 shows the stress contour of the shear connector at the collapse for L<sub>50</sub> specimen. The yielding in shear of the L-shaped shear connector is consistent with the experimental failure (Fig. 12).

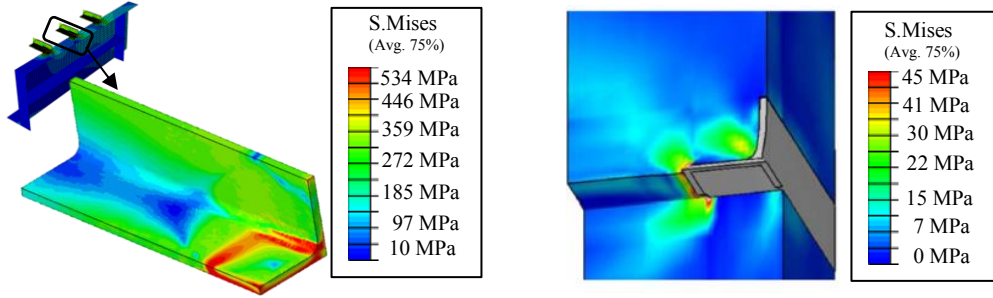


Fig. 15. Stress contours and deformed shape of the FE model for the L<sub>50</sub> specimen at collapse

A parametric study was then performed in order to determine a design equation for the L-angle shear connectors in the UCSB. Several key parameters that influence the behavior of the shear connectors such as material properties (concrete and shear connector), cross-section of shear connectors, and weld length are evaluated within this parametric study. At least three different variables are considered for each evaluated variable. It should however be noted that this parametric study was carried out on the model that was validated against the experimental results of the specimens with similar properties. Further validation of the model against experimental tests of different properties of the specimens would strengthen the conclusions of the numerical study.

The proposed equation is derived based on the observation of the deformation of shear connectors and of the stress pattern obtained from the FE simulation. As a consequence, the resistance of the shear connector is given by the shear resistance of the L-angle steel elements and an additional concrete contribution. The design formula is proposed as the following:

$$P_u = 2(A_{s1} + A_{s2}) \frac{f_u}{\sqrt{3}} + 2K_c A_c f_c \quad (1)$$

where  $A_{s1}$  and  $A_{s2}$  are the areas of the steel angle submitted to plastic shear at collapse (see Fig. 16),  $f_u$  is the ultimate stress of steel,  $A_c$  is the steel-concrete contact area of the part of the angle still connected to the U-shape steel profile at collapse,  $f_c$  is the resistance of the concrete in compression, and  $K_c$  is a calibration factor defined by the following expression obtained from a regression analysis of the parametric study:

$$K_c = 19 - 38 \frac{h_a}{H_c} \quad (2)$$

with  $h_a$  the height of the angle and  $H_c$  the height of the concrete slab. For more details, see [16].

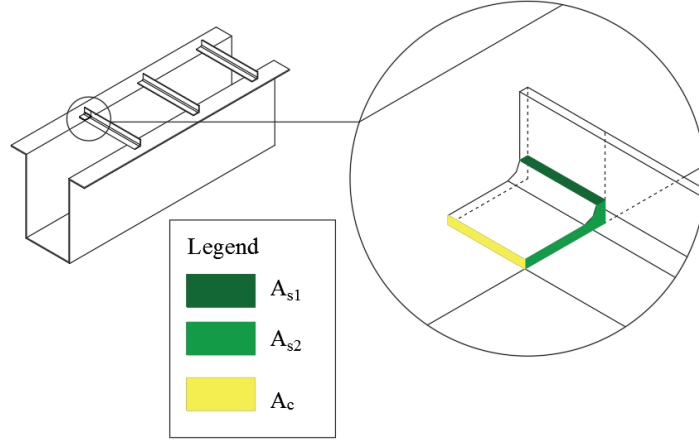


Fig. 16. Shear and concrete-steel contact areas

### 3.4 Formulation for shear force-slip relationship of the L-shaped shear connectors

For the specific case of the L<sub>50</sub> angles, the shear-force slip relationship can be defined based on the following expression [19]:

$$P = P_u(1 - \exp(-C_1\delta^{C_2})) \quad (3)$$

where  $C_1$  and  $C_2$  are calibration constants;  $P_u$  is the ultimate strength of the shear stud;  $\delta$  is the slip in millimeter.

This relationship has been adapted to fit with the shear-force slip curves of the L-angles obtained from the

experiment, which gives:

$$P = P_u(1 - \exp(-1.8\delta^{0.5})) \quad (4)$$

The comparison of the shear force-slip curves between the results obtained from the proposed expression and from the experimental test is illustrated in Fig. 17. A good agreement is achieved.

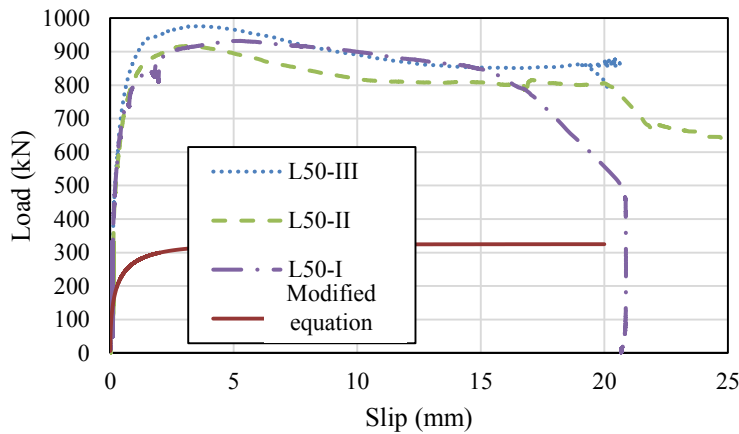


Fig. 17. Comparison of proposed force-slip relationship for L-shaped shear connector with the shear stud one.

## 4. Sagging behaviour of the UCSB

### 4.1 Experimental program

An experimental test was also carried out in order to investigate the sagging behaviour of the UCSB. The specimen is simply supported, as illustrated in Fig. 18. A vertical load is applied by a hydraulic jack onto a system of spreader beams in order to obtain a 4-point loading on the specimen. The longitudinal displacement of one of the vertical supports is restrained, and the torsion of the specimen is controlled by four guiding columns.

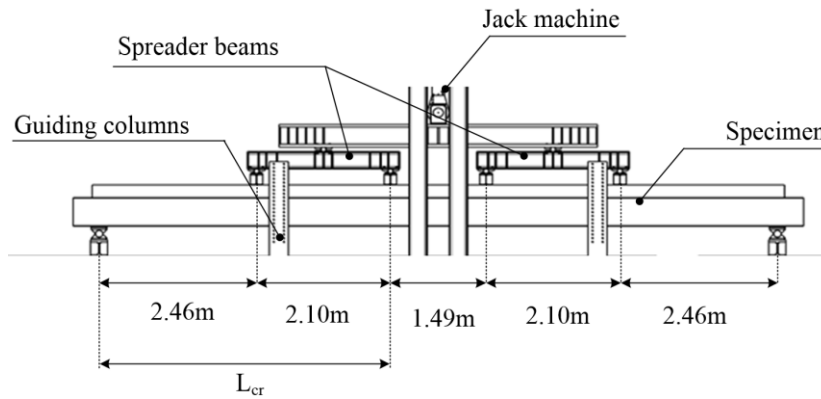


Fig. 18. Four point bending moment test setup (dimensions in m)

The cross-section of the specimen is the same as the one in the UCSB of the hybrid portal frame as seen in Fig. 5 (a)) except that the width of the concrete top slab is 2500mm and its height is 200mm. The longitudinal reinforcement bars are similar to the rebars of the central part of the hybrid frame (as seen in Fig. 5 (b)). The transversal reinforcement is composed of HA8 stirrups with a spacing of 430mm. The length of the specimen is 10600mm. Shear connectors with a dimension of 40x40x4mm and a spacing of 300 mm are used. Results of material characteristic tests are summarized in Table 3.

Table 3: Material properties

Concrete		U-shape		L-shape		Steel rebar	
Beam and slab	Precast Slab						
$f_{cm}$ (MPa)	$f_{cm}$ (MPa)	$f_y$ (MPa)	$f_u$ (MPa)	$f_y$ (MPa)	$f_u$ (MPa)	$f_y$ (MPa)	$f_u$ (MPa)
27	49	412	481	345	471	557	627

The degree of connection of the specimen in the test, denoted by  $\eta$ , is determined by the following expression:

$$\eta = \frac{nP_u}{Af_y} = 1.14 \quad (5)$$

where  $P_u$  is the resistance of the L-shaped shear connectors (see in Eq. (1)),  $n$  is the number of shear connectors welded on the critical length,  $A$  is the area of the U steel profile and  $f_y$  is the yielding resistance. The critical length  $L_{cr}$  is equal to the length between the maximum moment location and the support (Fig. 18). The interaction between steel and concrete is complete.

## 4.2 Numerical analysis

A finite element simulation of this test is performed using the software HBCOL. As this software was initially developed for hybrid columns, this simulation has the objective to confirm the validity of HBCOL software for UCSB elements under sagging moment. In order to perform an accurate comparison, stress-strain relationships are based on material characteristics. For steel rebars and U-shape profile, the stress-strain relationships is bi-linear and takes into account the strain hardening (Fig. 19 (a) and (b)). The model of concrete is based on EN1992-1.1 [9] and takes into account tensile resistance (Fig. 19 (c)). For shear connectors, the stress-strain relationship is based on Eq. (2) adapted on test results (Fig. 19 (d)).

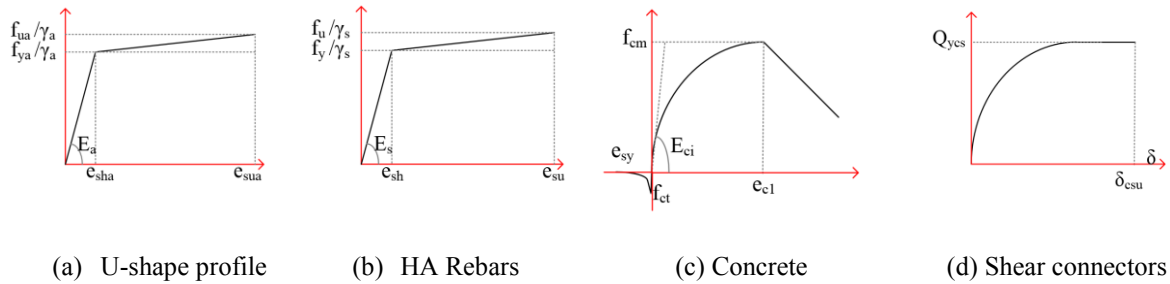


Fig. 19. : Strain stress relationship for UCSB components

The FE model is validated against the results obtained from the experimental test. A good agreement is obtained in the comparison of force-midspan displacement curves (Fig. 20.). Furthermore, a large plastic ductile behaviour of the specimen was observed (see Fig. 21). It should be noted that the test was stopped before failure due to the vertical misalignment on the jack machine.



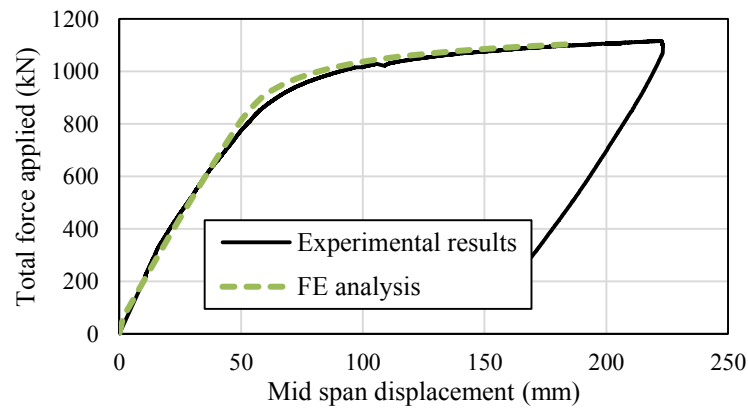


Fig. 20. Force-displacement curve at mid span



Fig. 21. Deflection of the beam after test

Fig. 22 presents the slips along the length of the beam obtained from the experiment and from the FE simulation.

250 The distribution of slips along the beam in the elastic behaviour (up to 800 kN) is similar between the two results.

The prediction is poor when the slips becomes large and some connectors begin to yield. Moderate slips between steel and concrete confirm the full connection of the UCSB in this test..

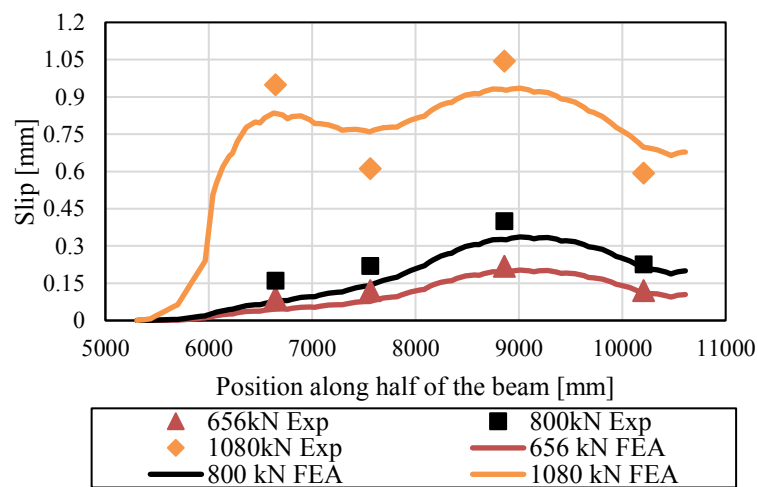


Fig. 22. Slip along the beam

Fig. 23 illustrates the longitudinal strain distribution on the mid-span cross-section. Strains in steel elements (positions in height from 200 to 700 mm) are parallel to those of the concrete (positions in height from 0 to 200 mm). This indicates that the curvatures in both materials are equal, which confirms that there is no uplift between the two materials and that the hypothesis of Bernoulli is valid.

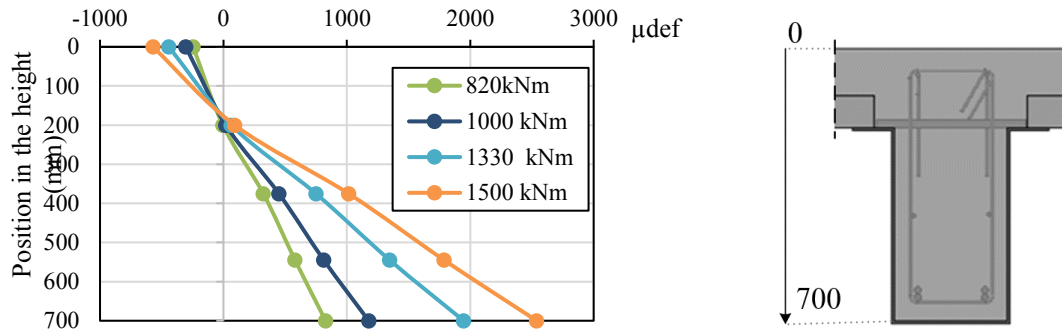


Fig. 23. Strain on the mid span section at different loading levels

### 4.3 Analytical model

Supposing that the Bernoulli hypothesis is applicable and the uplifts and slips are relatively small, an analytical model based on material laws and section properties of the specimen, similar to the one developed by Uy and Bradford [20], has also been developed in order to determine the moment-curvature curve. Fig. 24 shows a good agreement between the moment-curvature curves obtained from the analytical model, the FE model and the experimental tests.

The plastic bending moment is then determined from these curves using the method developed by Aribert & Lachal [21]. The values obtained are 1860 kNm for the analytical model, 1865 kNm for the FE model, and 1850 kNm for the experiment. It can be concluded that the behaviour of the UCSB under sagging bending moment can be determined with full connection between steel and concrete using the hypothesis of plane section.

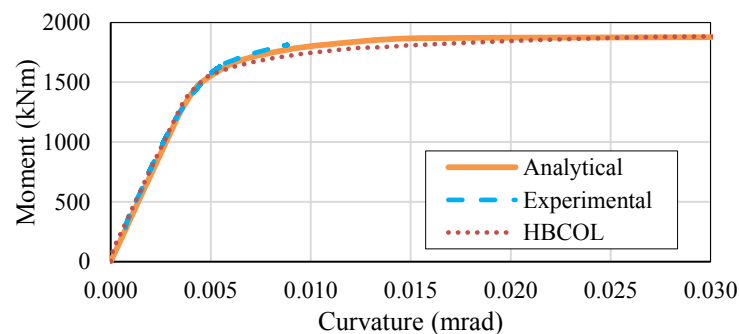


Fig. 24. : Moment-curvature curve at mid span

## 5. UCSB-to-column joint

### 5.1 Presentation

Whereas the UCSB is a hybrid section, in which bending moments in steel and in concrete have the same order of magnitude, in the composite column the resistance is mainly provided by the steel cross-section. As a consequence, load transfers between materials must be ensured. To achieve that, different steel pieces are welded to the steel beam and to the steel column, and encased in the concrete, as shown in Fig. 25 (a). The continuity of the steel is made by inserting the steel column through a hole of the U-shape steel beam, and fixing the two members together by welds on the edges that are in contact as seen in Fig. 25 (b). The continuity of the inside concrete element from the beam to the column is ensured by longitudinal rebars that cross the inner flange of the column through a V-shape hole.

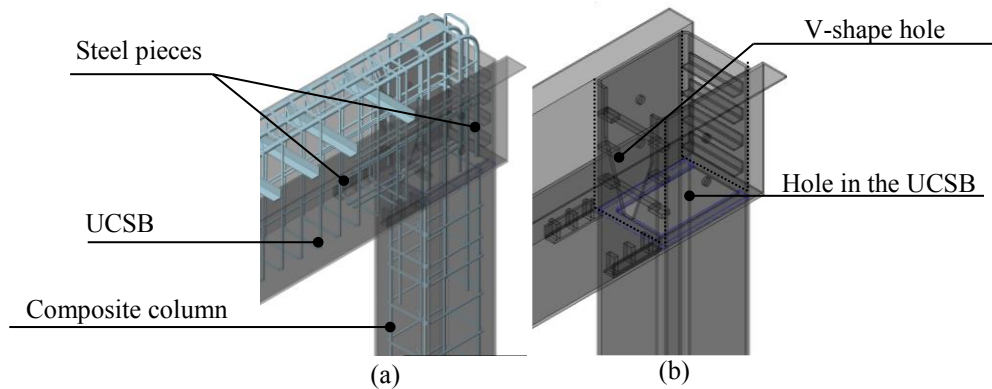


Fig. 25. Details of the hybrid joint: (a) with steel rebars (b) without steel rebars

The initial design of the joint was made by an analytical model based on a strut and tie model of the concrete part combined with a shear panel type model of the steel part. However, since the behaviour of the UCSB-to-column hybrid joint is crucial to the global structural behaviour of the frame, four full-scale experimental tests of the joint have been performed in order to verify the design. The moment resisting capacity and the failure mode of the joint are obtained and presented in the next section. In order to gain more insights on the force transfer within the joint, a finite element model has been developed in Abaqus [22]. Then, the validation of the analytical design model is made by analyzing the observations made during the experimental tests, and the results from the FE simulation.

5.2.1 Experimental setup

An experimental program is carried out on two specimens ( $M_2$  and  $M_3$ ) in order to verify the behaviour of the joint. The test specimen is composed of the composite column and the hogging zone of the UCSB. Therefore, it validates also the behaviour of the UCSB under negative bending moment. The dimensions of the cross-sections of these members are the same as the ones of the portal frame. The lengths of the column and of the beam are 2.845m and 1.5m, respectively. The width of the concrete slab is 1100 mm. Results of material characteristic tests are summarized in Table 4.

Table 4: Materials properties

	Concrete		U-shape		Column		L-shape		Steel rebar	
	Beam and slab	Precast								
	$f_{cm}$	$f_{cm}$	$f_y$	$f_u$	$f_y$	$f_u$	$f_y$	$f_u$	$f_y$	$f_u$
$M_2$	31	41	422	503	517	535	330	471	580	640
$M_3$	30.7									

The configuration of the test setup is illustrated in Fig. 26 (a) and described as following. The specimen is rotated by 90 degrees. The supports at the column base and at the end of the UCSB are hinged. A system of rigid steel elements that is fixed to the pin and in contact with the concrete slab is designed so that the applied shear force is distributed to both the steel and the concrete elements (see Fig. 26 (b)). A horizontal load is applied to the end of the UCSB by a hydraulic jack in order to produce the hogging bending moment.

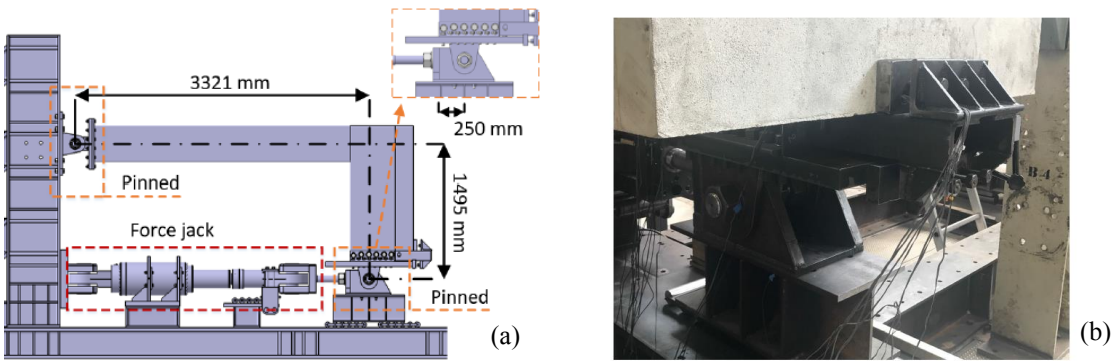


Fig. 26. Test setup for the hybrid joint (a) global schema (b) details of the rigid element

The photo of the specimen  $M_2$  after the test is presented in Fig. 27. The failure of the specimen was governed by the plastic buckling of the bottom flange of the steel column. Observations were similar in specimen  $M_3$ .



Fig. 27. Beam-column joint after collapse

The moment-rotation curve is illustrated in Fig. 28. The moment in this figure was computed at the intersection of the neutral axis of the beam and of the column, whereas the rotation is computed by using the data obtained from the displacement sensors. The classification of the joint can be determined based on EN1993-1.8 [23] for its ductility, stiffness and resistance. As the maximum rotation of the joint within the two tests is larger than 0.04 rad, the hybrid joint is classified as ductile.

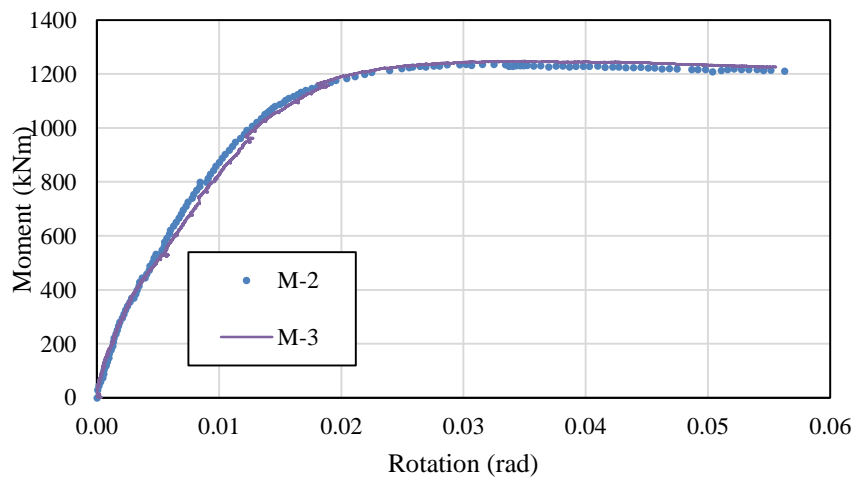


Fig. 28. Rotation-bending moment diagram

Table 5 gives the values of the plastic moments ( $M_y$ ), elastic bending moment ( $M_{el}$ ), and the initial stiffness of  
 310 the joint ( $S_{j,ini}$ ) of each specimen. These values are determined using the method developed by Aribert & Lachal  
 [21] described in Fig. 29.  $M_{el}$  is taken as equal to 2/3 of  $M_y$  and ( $S_{j,ini}$ ) corresponds to  $M_{el}$ .

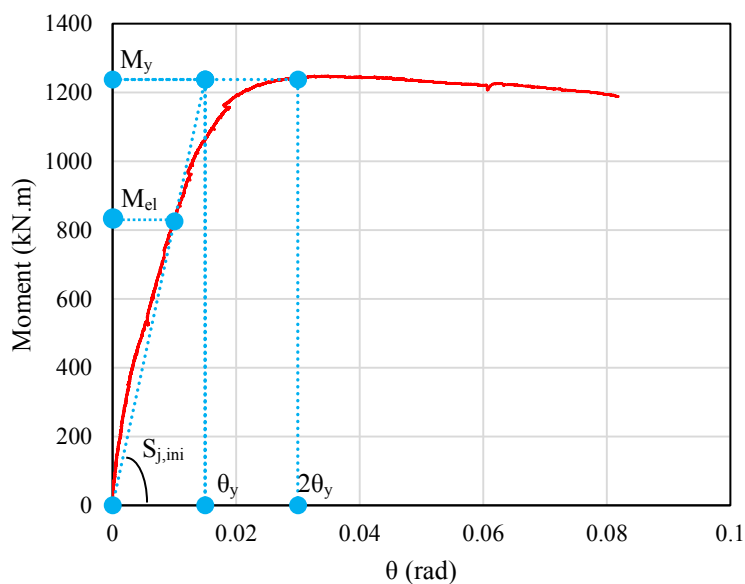


Fig. 29. Determination of  $M_y$  and  $\theta_y$  by Aribert and Lachal method

Table 5 : Determination of plastic resistance and initial stiffness

Specimen	$M_2$	$M_3$
$M_y$ (kNm)	1232	1237
$M_{el}$ (kNm)	823	830
$S_{j,ini}$ (kNm/rad)	90113	86395

315 In the AVRIL project, the acting bending moment at ULS is equal to 798 kNm. The mean value of the resisting  
 bending moment obtained from the experimental tests is 1235 kNm. Then, the UCSB-to-column joint can be  
 considered as fully resistant.

The limits for classifying the rigidity of the joint can be determined based on EN1993-1.8[23]. They depend on  
 the length of the beam and its flexural stiffness. In the case of the AVRIL portal frame, the limits to classify the  
 320 joint as rigid or as pinned are equal to 272000 kNm/rad and 5400 kNm/rad, respectively. Consequently, the hybrid  
 joint can be regarded as semi-rigid.

### 5.3 FE validation

A full finite element model was also made with Abaqus in order to acquire more information about the distribution of the stresses within the joint. Explicit general contact interaction was used to define the contact behavior of the concrete parts with the U-shape steel profile, the steel tube column and the other steel pieces. The interface between the onsite cast and the precast concrete slabs was not modelled. All the important components in the specimen are included, and the model is simulated in half with respect to a symmetric condition, see Fig. 30. The inside concrete beam and concrete column are modelled by solid element type C3D10 whereas the U-shape profile and the steel column tube are meshed using shell element type S4R. 2-node beam element B31 and solid element type C3D8R were used for the steel rebars and other steel components in the joint, respectively. A concrete model with material softening presented in [24] was used in the present simulation and the actual stress-strain curves obtained from coupon tests were used for the material model for steel elements.

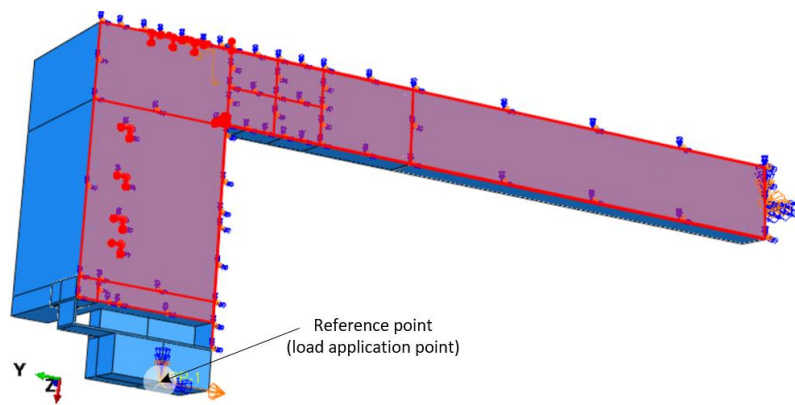


Fig. 30. FE model of the beam to column joint

The following paragraph presents only the validation of the FE model in comparison with the experimental results. The full description of the FE model and its hypotheses are presented in a next paper.

To validate the FE model, the global as well as the local behaviour of the joint are studied by comparing the results obtained from the experiment with those from the FE simulation. Firstly, the bending moment versus rotation curves are compared, and a good match between the pair is achieved as presented in Fig. 31. Secondly, in the FE model, the failure is also governed by the buckling of the column lower flange.

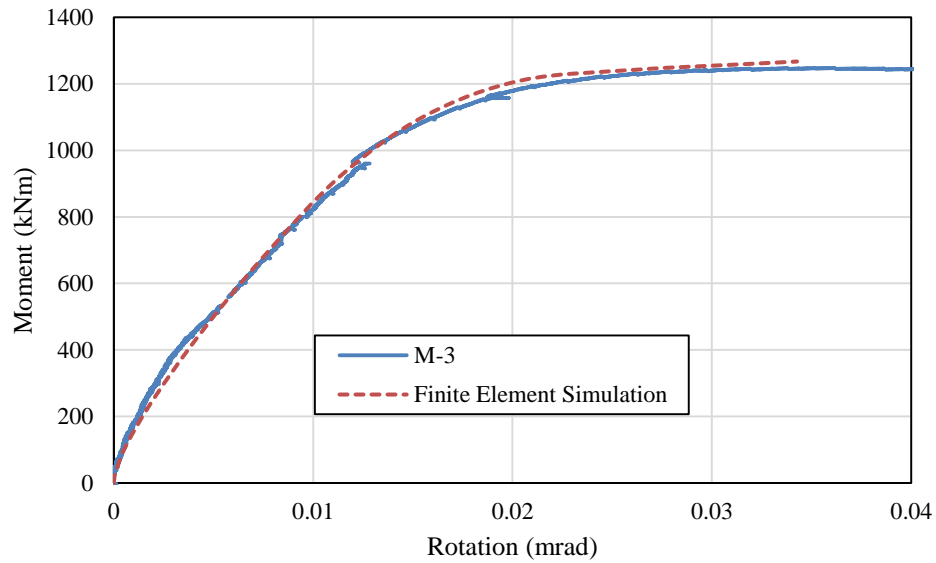


Fig. 31. Moment rotation curves

In order to validate the numerical distribution of forces within the joint, the plastic stain pattern obtained from the FE model and the cracks observed in the specimen after the test were compared and a good match is obtained as seen in Fig. 32. **It should be however noted that this validation is made only on test specimens with the properties of the AVRIL project. More experimental tests on specimens with different geometries should be done in order to generalize the model.**

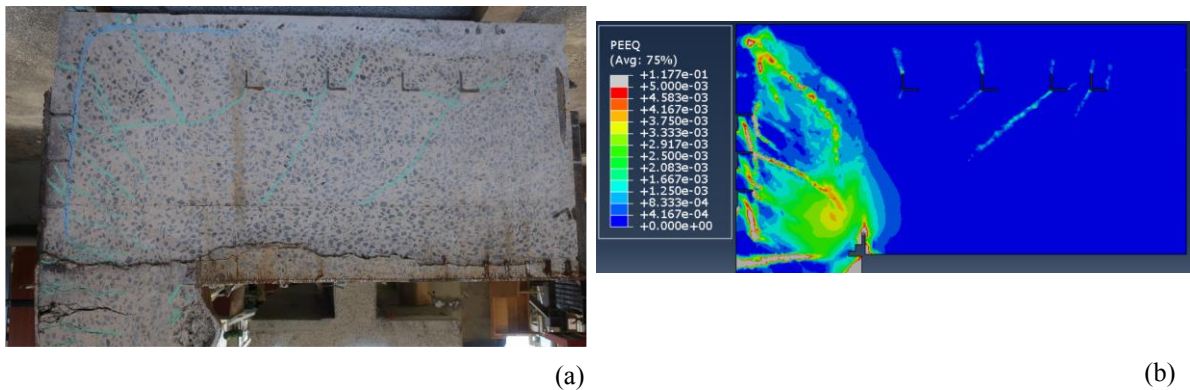


Fig. 32. Section cut: (a). Cracking patterns in specimen (b). Plastic strain PEEQ of FE model.

## 6. On-site application: specific detailing and feedbacks

### 6.1 UCSB-to-UCSB joint

As explained in the introduction, the steel portal frame is prefabricated in three parts that are not connected on site by any bolt or weld. It is only the concrete casting that ensures the continuity of the beam. Joints are located



near inflection points of the bending moment diagram under permanent loads. To ensure an easy setup, a gap of 1cm between the steel parts is left.

350 In order to obtain the values of the forces in the joint, nonlinear structural analysis of the portal frame have been cautiously extended by a large parametrical study taking into account the live load variation, possible geometrical imperfections, an eventual settlement of column bases, and different levels of stiffness of the beam-to-column joint. The envelope curve of the bending moments at ULS is presented in Fig. 33. The study is made over the left joint. Moreover, a supplementary safety factor of 1.4 has been applied in the design of the joint in  
355 order to make this critical zone over resistant.

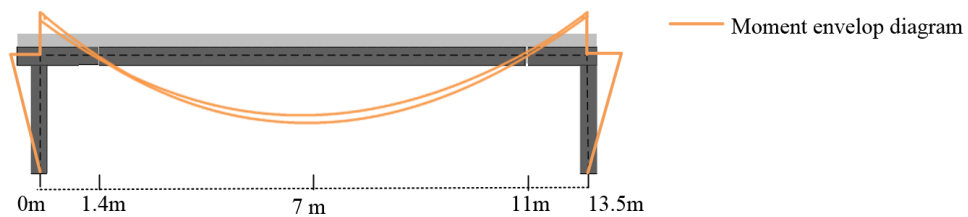


Fig. 33 Location of Inflection points and UCSB-to-UCSB joints

The joint is composed of two sides. The end of the outer beam is called side A and the end of the central part side B as illustrated in Fig. 34. In Side A, the joint contains five stiffeners and two additional L-angles. In side B, the joint consists of two protruding UPNs, two lower L-angles, one L-angle tie and two additional L-angles. The detailed dimensions of all the components are given in Appendix A.  
360

The transfer of steel shear forces from side B to the steel section of side A is made from the 2 protruding UPN profiles welded on the webs of the beam of side B to the stiffeners welded on the bottom flange of the beam of side A by the concrete.

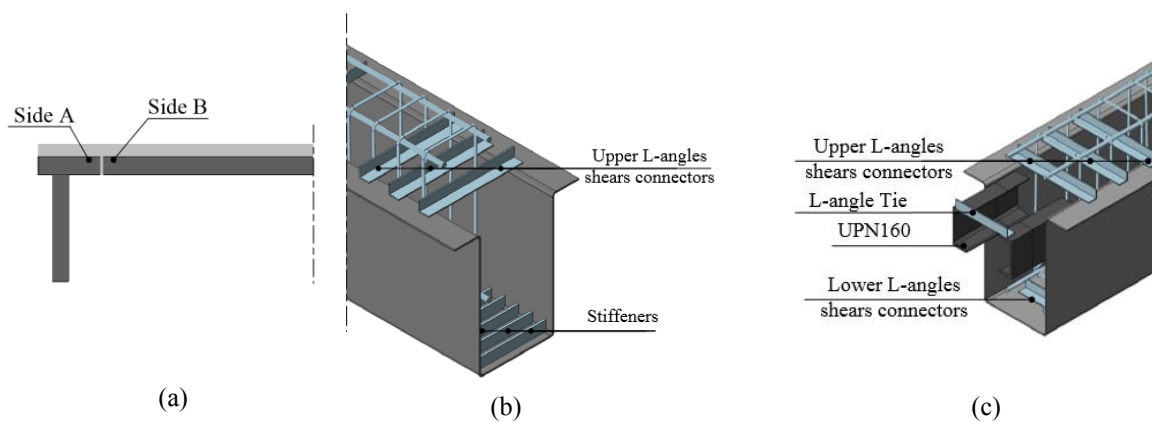


Fig. 34. UCSB-to-UCSB joint: (a) Location of the two sides. (b) Side A. (c) Side B.

The transfer in the concrete beam of the longitudinal forces in the upper and lower flanges of the U-shape section is ensured by additional L-angle shear connectors or stiffeners welded to the flanges on both sides of the  
365

joint. The additional tension transmitted in the concrete is resisted by two additional reinforcing cages overlapping the joint, see Fig. 35.

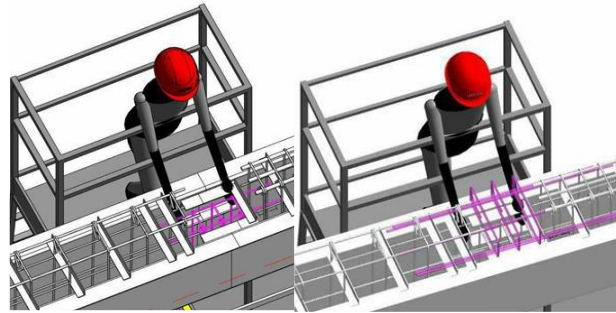


Fig. 35. Additional cages at inflection point : lower cage (a) and upper cage (b)

Although all the components of the joint can be designed using Eurocodes [9,10,11], it was decided that two experimental tests of the UCSB-to-UCSB joint would be performed. The results from the tests have shown an over-resistance of the joint as the failure of the joint was attained at a maximum load that is equal to three time the ULS load. The failure mode of the specimens was governed by the yielding of the tensile steel reinforcement bars. The detail of these tests is not presented here.

## 6.2 Column base joint

The connection at the column base has also to be fast and easy without any bolts or welds. Consequently, this joint has been designed as a hinge. In this perspective, four L-angles are welded to the inner surface of the steel column (Fig. 36). After casting, these L-angles transfer stresses from the steel to the infilled concrete member so that the connection is made only by the inside concrete column.



Fig. 36. Column shoe connection

### 6.3 Feedback of the on-site erection

The AVRIL building is the first project where the hybrid portal frame was set up. The steps of the erection of the hybrid frame (Fig. 37) were as follows:

- Positioning, aligning and shoring of 2 outers parts;
- Insertion of the inner part with intermediate shoring;
- Setting up of steel reinforcing cages at inflection joint;
- Casting of columns and U-beam drop with a self-compacting concrete;
- Setting and shoring of precast concrete slabs;
- Casting of concrete slab.

As the system was considered to save time on site, the feedback of workers was of primary importance. They enjoyed the hybrid frame, as steel elements are easier to handle than prestressed members. As a consequence, the assembly is fast and secure. These new elements have increased the set up throughput.



Fig. 37. Erection of the steel portal frame

## 7. Conclusions

On the basis of a U-shape steel profile used as permanent formwork, an innovative concrete-steel hybrid beam, named as U-shape concrete steel beam (UCSB) has been developed. The U-shape steel profile acts as a composite beam with the slab, while the infill concrete acts as a classical concrete beam. The connection of the U-shape steel profile is made by angle connectors welded on the upper flanges of the profile. This system is able to reach large spans similar to the ones of prestressed members, while being lighter and easier to set up.

This system has been used in a pilot project, the AVRIL R&D center near Rennes. It was taken advantage of the duality of the UCSB to make the on-site joints only by the concrete beam, allowing an assembly without any

weld or bolt on site. This successful pilot project confirms the applicability in actual buildings and its economic interests.

400 The structural analysis and design has been made using a specific software called HBCOL and the design of the joints by models based on the strut and tie method. As the UCSB and the specific detailing adopted in the joints are not covered in present norms, experimental validations were required. A series of full-scale experimental tests have been performed in order to assess the global and local behaviour of the frame, its connections and design models have been deduced:

405 - The shear resistance of the L-angle connectors inside the UCSB has been determined by 4 asymmetrical push-out tests. These tests have been used to validate a detailed FE model. A numerical parametric study has led to a proposition of an analytical expression for the shear resistance of the L-angle connectors in UCSB.

- One 6-point bending test has been made in order to investigate the resistance of the UCSB under sagging bending moment. It was used to validate the relevance of the software HBCOL.

410 - Two tests have also been carried out in order to confirm the design of the on-site joints

- Finally, four tests of the beam-to column joint were performed, and a finite element model was validated by comparison to the experimental results. The plastic strain pattern obtained from the simulation and the observation of the cracks in the specimens were used to refine the analytical design model of the joint. It should be however noted that the scope of the current experimental tests is limited on specimens with the same properties from AVRIL project. More experimental tests on different geometries of the specimens would strengthen the conclusions of this study.

415 An approval has been obtained from the CSTB, the French certification organism, for the design procedure of the members and of the joints has obtained.

## Acknowledgements

420 The authors gratefully acknowledge financial support by the ANR (Agence Nationale de la Recherche, France) through the project LabCom ANR B-HYBRID.

## References

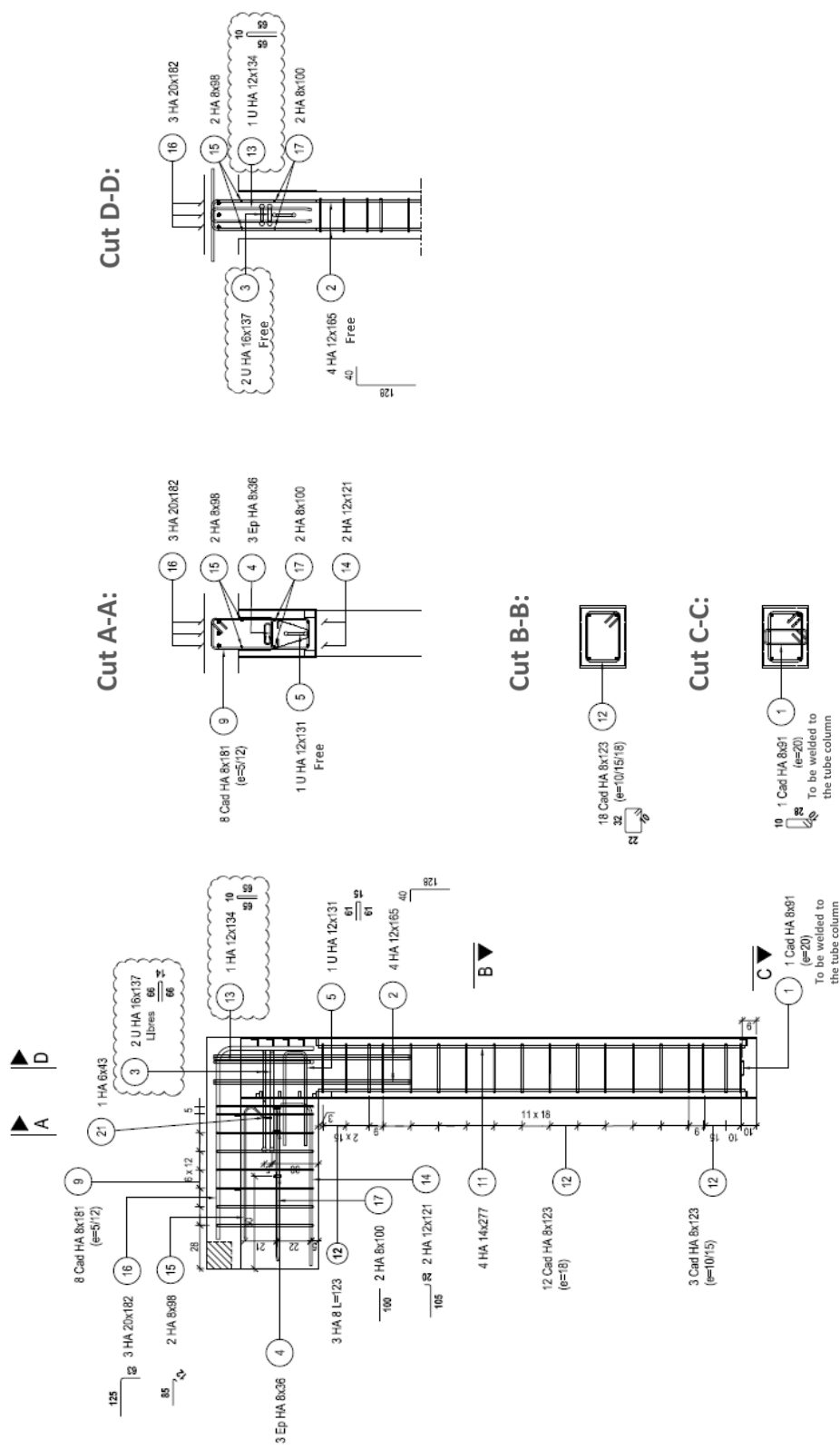
- [1] R. G. Slutter, G. C. Driscoll Jr, Flexural strength of steel and concrete composite beams, Tech. Rep., Fritz Engineering Laboratory-Lehigh University, 1963.
- 425 [2] B. Uy, M. A. Bradford, Ductility of profiled composite beams: Part I Experimental study, Journal of Structural Engineering 121 (5) (1995) 876-882.
- [3] B. Uy, M. A. Bradford, Ductility of profiled composite beams: Part II Analytical study, Journal of Structural Engineering 121 (5) (1995) 883-889.
- [4] S. Nakamura, Bending behaviour of composite girders with cold formed steel U section, Journal of  
430 Structural Engineering 128 (9) (2002) 1169-1176.
- [5] H.-G. Park, H.-J. Hwang, C.-H. Lee, C.-H. Park, C.-N. Lee, Cyclic loading test for concrete-filled U-shaped steel beam RC column connections, Engineering Structures 36 (2012) 325-336.
- [6] L.-H. Chen, S.-T. Li, H.-Y. Zhang, X.-F. Wu, Experimental study on mechanical performance of  
435 checkered steel-encased concrete composite beam, Journal of Constructional Steel Research 143 (2018) 223-232.
- [7] Liu Y, Guo L, Qu B, Zhang S. Experimental investigation on the flexural behavior of steel-concrete composite beams with U-shaped steel girders and angle connectors. Engineering Structures 2017; 131:492–502.
- [8] Keo P, Somja H, Nguyen QH and Hjjaj M. Simplified design method for slender hybrid columns. Journal  
440 of Constructional Steel Research 2015; 110:101-120
- [9] CEN. Eurocode 2: EN 1992-1-1 Design of concrete structures, Part 1.1 – General Rules for buildings. Brussels; 2004
- [10] CEN. Eurocode 3: Design of steel structures -Part 1-1: General rules and rules for buildings (NF EN 1993-1-1). Brussels; 2003.

- 445 [11]CEN. Eurocode 4: EN 1994-1-1 Design of composite steel and concrete structures, Part 1.1– General Rules for buildings. Brussels 2004.
- [12]I.M. Viest, Investigation of stud shear connectors for composite concrete-steel T-beams, J. Am. Concr. Inst. 27 (8) (1956) 875–891.
- [13]D. Lam, E. El-Lobody, Behavior of headed stud shear connectors in composite beam, J. Struct. Eng. 131 (1) (2005) 96–107.
- 450 [14]H.T. Nguyen, S.E. Kim, Finite element modeling of push-out tests for large stud shear connectors, J. Constr. Steel Res. 65 (10) (2009) 1909–1920.
- [15]J. Nie, Y. Xiao, L. Chen, Experimental Studies on Shear Strength of Steel-Concrete Composite Beams, Journal of Structural Engineering 130 (8) (2004) 1206-1213.
- 455 [16]Keo P, Lepourry C, Somja H, Palas F. Behavior of a new shear connector for U-shaped steel-concrete hybrid beams, Journal of Constructional Steel Research 145 (2018) 153–166.
- [17]Chinn J. Pushout Tests on Lightweight Composite Slabs. AISC Engineering Journal 1965, 2(4) 129-134
- [18]Lowe D, Das R, Clifton C. Characterization of the Splitting Behavior of Steel-concrete Composite Beams with Shear Stud Connection. Procedia Mater Sci 2014; 3:2174–2179.
- 460 [19]Hanswille G, Pörsch M, Ustundag C. Resistance of headed studs subjected to fatigue loading. J Constr Steel Res 2007 ;63 :485-93.
- [20]Uy, B, and Bradford, M. A. (1993a). "Cross-sectional deformation of prestressed composite tee-beams." Struct. Engrg. Rev., 5( 1). 63- 70.
- [21]J-M. Aribert & A. Lachal,. (2002), Formulation de la rupture par fatigue de connecteurs acier-béton pour des sollicitations de type sismique: Application aux assemblages. Construction Métallique. Retrieved from <http://cat.inist.fr/?aModele=afficheN&cpsidt=16604864>.
- 465 [22]Abaqus documentation, version 6.14, Dassault system,2014.
- [23]EN 1993-1-8, Eurocode 3: Design of steel structures: Part 1-8: Design of joints, European Committee for Standardization, 2005.
- 470 [24]B. Alfarah, F. Lopez-Almansa, S. Oller, New methodology for calculating damage variables evolution in plastic damage model for RC structure, Engineering structures 132 (2017) 70-86.
- [25]Brandonisio G, De Luca A, Mele E, Shear strength of panel zone in beam-to-column connections, Journal of Constructional Steel Research 71 (2012) 129–142.

- [26] Mou B, Pang, L, Qiao Q, Yang Y; Experimental investigation of unequal-depth-beam-to-column joints with t-shape connector; *Engineering Structures* 174 (2018) 663–674.
- [27] Mou B, Bai Y; Experimental investigation on shear behavior of steel beam-to-CFST column connections with irregular panel zone, *Engineering Structures* 168 (2018) 487–504.
- [28] G. Loho, A. Lachal, Modelling of strengthened column web panel in bolted end-plate composite joints, *Journal of Constructional Steel Research* 64 (2008) 584–595.

Appendix A

Outer Part I : Steel reinforcement

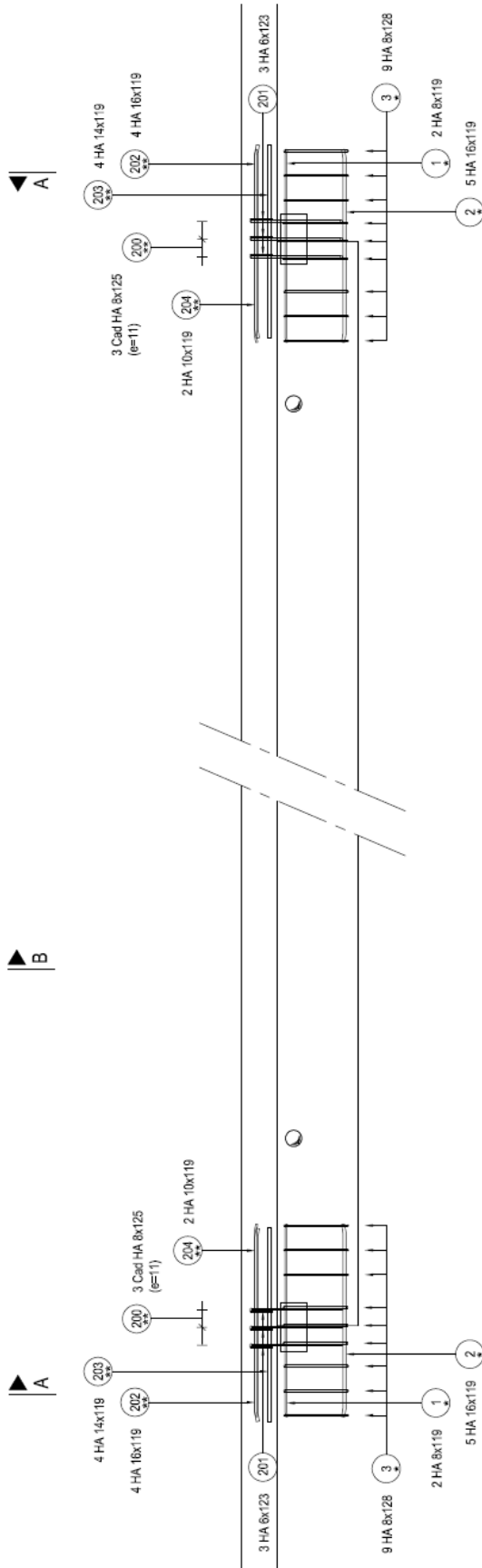




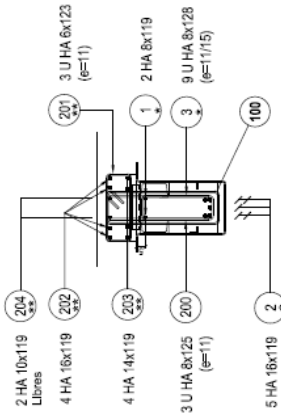
## List of rebars - shape

Pos.	Steel grade	$\phi$ [mm]	Pieces	No. ele.	No. Total	Esp.	Individual length [m]	Calculated shape (non scale)	Total length [m]	Weight [kg]	
1	HA	8	1	1	1	0,20	0,91		0,91	0,36	
2 Ind,A	HA	12	4	1	4	0,16	1,65		6,60	5,86	
3	HA	10	2	1	2		1,41		2,83	1,74	
4	HA	8	3	1	3		0,36		1,07	0,42	
5	HA	12	1	1	1	0,04	1,31		1,31	1,17	
9 Ind,A	HA	8	8	1	8	0,12	1,81		14,47	5,71	
11	HA	14	4	1	4		2,84		11,34	13,73	
12	HA	8	18	1	18	###	1,23		22,11	8,73	
13	HA	12	2	1	2	0,16	1,46		2,93	2,60	
14	HA	12	2	1	2		1,21		2,42	2,15	
15	HA	8	2	1	2		0,98		1,96	0,77	
16	HA	20	3	1	3		1,82		5,46	13,45	
17	HA	8	2	1	2		1,00		2,00	0,79	
21	HA	6	1	1	1	0,12	0,43		0,43	0,09	
Average $\phi$		11.1							Total :	75.84	57.57

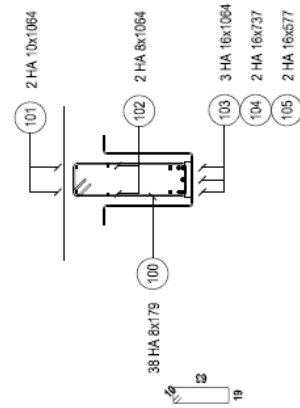
***Central part : Steel reinforcement***



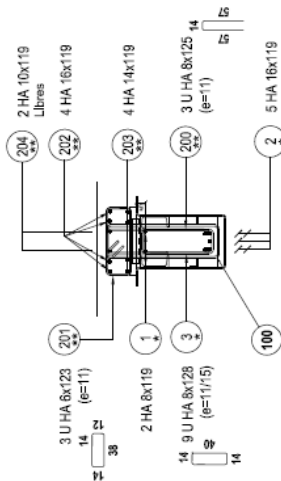
Cut A-A:

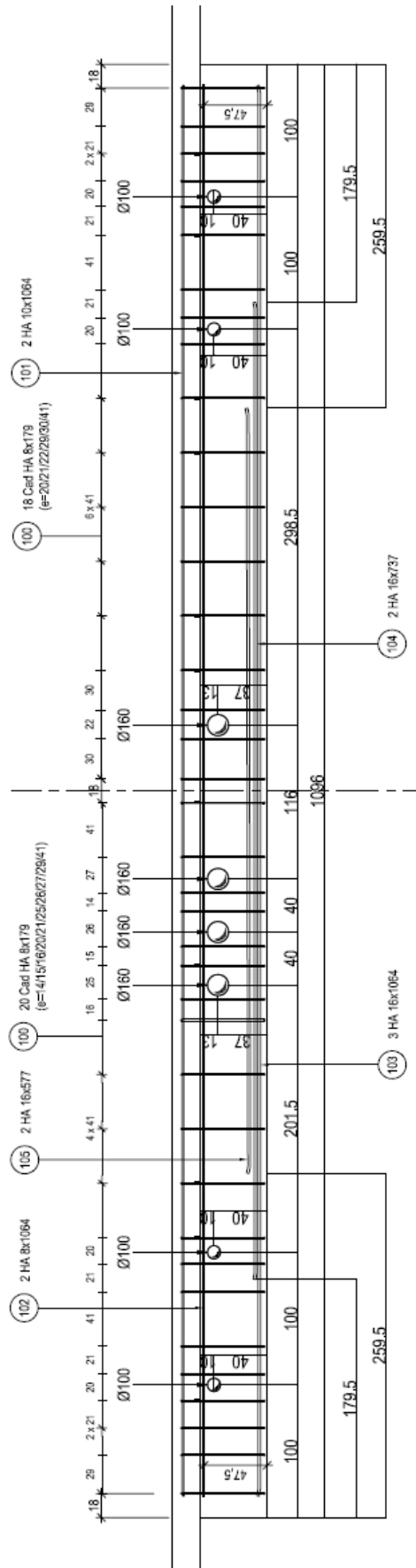


**Cut B-B:**

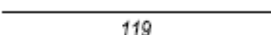
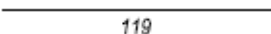
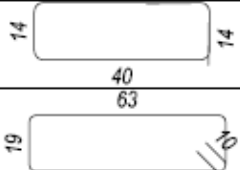

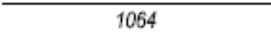
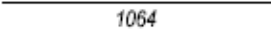
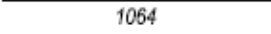
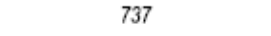

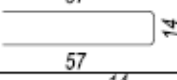
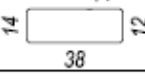
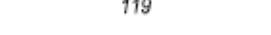
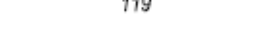
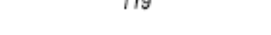


Cut A-A:

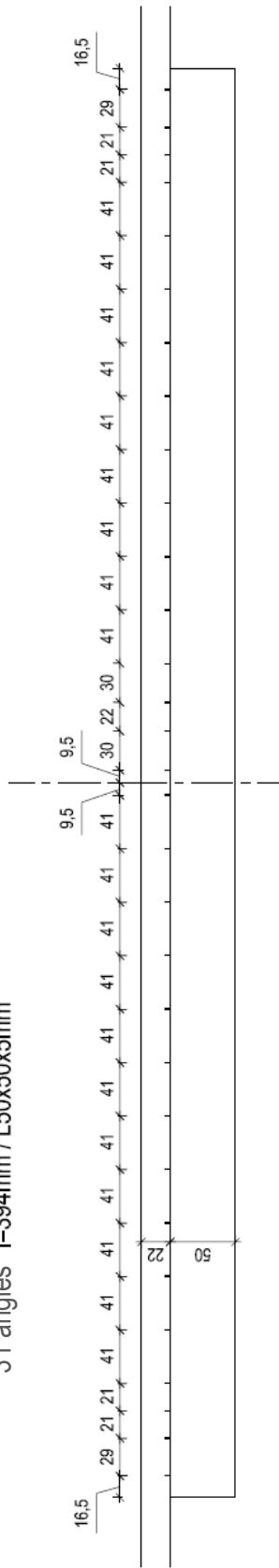




## List of rebars - shape

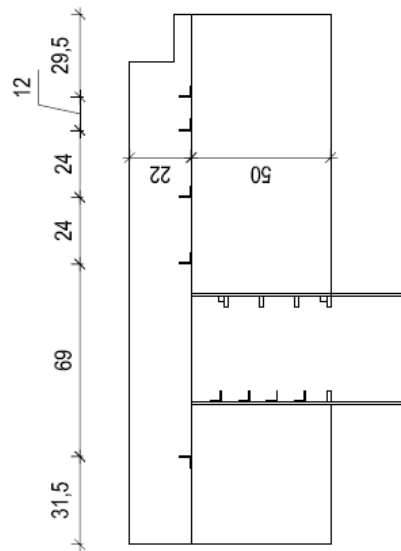
Pos.	Steel grade	$\phi$ [mm]	Pieces	No. ele.	No. Total	Esp.	Individual length [m]	Calculated shape (non scale)	Total length [m]	Weight [kg]	
1	HA	8	4	1	4		1.19		4.77	1.88	
2	HA	16	10	1	10		1.19		11.93	18.85	
3	HA	8	18	1	18	###	1.28		22.96	9.07	
100	HA	8	38	1	38	0.41	1.79		68.11	26.91	
101	HA	10	2	1	2		10,64		21.28	13.13	
102	HA	8	2	1	2		10,64		21.28	8.41	
103	HA	16	3	1	3		10,64		31.92	50.43	
104	HA	16	2	1	2		7,37		14,74	23,29	
105	HA	16	2	1	2		5.77		11.54	18.23	
200	HA	8	6	1	6	0.11	1.25		7.49	2.96	
201	HA	6	6	1	6	0.11	1.23		7.36	1.63	
202	HA	16	8	1	8		1.20		9.56	15.10	
203	HA	14	8	1	8		1.20		9.56	11.57	
204	HA	10	4	1	4		1.19		4.77	2.94	
Ø moyen		11.6							Totaux:	247.27	204.40

31 angles l=394mm / L50x50x5mm



**Cut PB xxxa:**

5 angles l=394mm / L50x50x5mm



**Cut PB xxxc:**

4 angles l=394mm / L50x50x5mm

